Earthq Eng & Eng Vib (2018) 17: 555-566 **DOI**: https://doi.org/10.1007/s11803-018-0462-9

Finite element response sensitivity analysis of three-dimensional soil-foundation-structure interaction (SFSI) systems

Gu Quan[1†], Liu Yongdou[1‡], Li Yong[2§] and Lin Chun[1‡]

1. *School of Architecture and Civil Engineering, Xiamen University, Xiamen 361005, Fujian, P.R. China*

2. *Department of Civil and Environmental Engineering, University of Alberta, Edmonton, T6G 1H9, Canada*

Abstract: The nonlinear finite element (FE) analysis has been widely used in the design and analysis of structural or geotechnical systems. The response sensitivities (or gradients) to the model parameters are of significant importance in these realistic engineering problems. However the sensitivity calculation has lagged behind, leaving a gap between advanced FE response analysis and other research hotspots using the response gradient. The response sensitivity analysis is crucial for any gradient-based algorithms, such as reliability analysis, system identification and structural optimization. Among various sensitivity analysis methods, the direct differential method (DDM) has advantages of computing efficiency and accuracy, providing an ideal tool for the response gradient calculation. This paper extended the DDM framework to realistic complicated soil-foundation-structure interaction (SFSI) models by developing the response gradients for various constraints, element and materials involved. The enhanced framework is applied to three-dimensional SFSI system prototypes for a pile-supported bridge pier and a pile-supported reinforced concrete building frame structure, subjected to earthquake loading conditions. The DDM results are verified by forward finite difference method (FFD). The relative importance (RI) of the various material parameters on the responses of SFSI system are investigated based on the DDM response sensitivity results. The FFD converges asymptotically toward the DDM results, demonstrating the advantages of DDM (e.g., accurate, efficient, insensitive to numerical noise). Furthermore, the RI and effects of the model parameters of structure, foundation and soil materials on the responses of SFSI systems are investigated by taking advantage of the sensitivity analysis results. The extension of DDM to SFSI systems greatly broaden the application areas of the d gradient-based algorithms, e.g. FE model updating and nonlinear system identification of complicated SFSI systems.

Keywords: finite element method; response sensitivity analysis; direct differentiation method; finite difference method; soil-foundation-structure interaction

1 Introduction

Finite element (FE) analysis has become a powerful tool for design and analysis of structural and/or geotechnical systems. Therefore, significant research efforts have been devoted to the development of nonlinear FE models for structural components or devices (Perić *et al*., 1992), as well as the complex civil infrastructure systems (Ueno and Liu, 1987; Karoumi, 1999).

The response sensitivities to various model parameters, such as material parameters, geometric parameters and loading parameters, are of significant importance in many other subfields of structural engineering using gradient-based algorithms. These subfields include simplified probabilistic response analysis for performance assessment (Singhal and Kiremidjian, 1996; Kunnath *et al*., 2006; Dolšek and Fajfar, 2007), finite element model updating (Ditlevsen and Madsen, 1996; Kleiber *et al*., 1997), system identification (Haber and Unbehauen, 1990; Nelles, 2001), health monitoring (Doebling *et al*., 1996), structural reliability (Zou *et al*., 2000), structural control, and structural optimization (Yao, 1972). Besides, the stand-alone response sensitivity analysis also plays a significant role in determining the effects and relative importance (RI) of loading/model parameters with regard to the system responses(Conte, 2001; Conte *et al*., 2003, 2004; Gu and Conte, 2003; Zoutat *et al*., 2016; Yang *et al*., 2017; Zdeněk and Valeš, 2017; Fielder *et al*., 2017).

A variety of response sensitivity analysis methods have been developed, including the Perturbation Method (PM) (Kleiber and Hien, 1992), the Adjoint Method (AM) (Kleiber *et al*., 1997), the Finite Difference Method

Correspondence to: Li Yong, Department of Civil and Environmental Engineering, University of Alberta, Edmonton, T6G 1H9, Canada
Tel: +1-780-492-2722
E-mail: yong9@ualberta.ca
[†]Professor; [‡]Graduate Student; [§]Assistant Professor

Supported by: National Key Research and Development Program of China under Grant No. 2016YFC0701106, Natural Sciences and Engineering Research Council of Canada via Discovery under Grant No. NSERC RGPIN-2017-05556 Li
Received November 20, 2016; **Accepted** September 21, 2017

(FDM) (Kleiber *et al*., 1997; Conte *et al*., 2003), and the Direct Differentiation Method (DDM) (Keliber *et al*., 1997; Conte, 2001; Conte *et al*., 2003; Gu and Conte, 2003; Barbato and Conte, 2005; Zona *et al*., 2005). Among these methods, DDM is general and applicable to a wide range of material constitutive models. This makes DDM either outperform the other methods in terms of accuracy, due to numerical noise or approximation (e.g., FDM, PM), outperform the other methods in terms of computational efficiency (e.g., FDM) or being beyond the limitation to elastic systems (e.g., AM). However, DDM has not been extended to complicated 3D soil-foundation-structure interaction (SFSI).

The main contribution of the paper is to bridge this gap by extending state-of-the-art FE algorithms for response-only computation to the response sensitivity analysis. The newly developed algorithms are implemented in a general FE analysis framework, OpenSees (an Open system for earthquake engineering simulation, Mazzoni *et al*., 2004, 2006), based on which the authors have contributed significantly to the DDM framework for accommodating various constraints, elements, materials, and analysis techniques (Gu *et al*., 2008, 2009, 2011, 2013, Ciampoli and Pinto, 1995). In this paper, two 3D SFSI systems (i.e., one for a prototype of pile-supported bridge pier column and the other for pile-supported frame building) subject to uniform earthquake ground motion excitation are investigated. Response sensitivities of SFSI systems are computed with respect to parameters associated with the material models in structure (e.g., concrete, steel), foundation and soils are studied in detail. Forward finite difference method (FFD) is used to verify the accuracy of the DDM based response sensitivities. Effects and relative importance of the model parameters with regard to different response quantities of interest in the SFSI systems is also explored.

2 Sensitivity analysis using DDM

In the nonlinear FE method, a generic scalar response quantity r can be considered as an implicit function of model parameters θ (e.g., geometric, material, or loading parameters), and the function is represented by a nonlinear FE model,

$$r = f(t,\theta) \tag{1}$$

The response sensitivity is defined as the partial derivative of r with respect to parameter θ, $\partial r/\partial\theta = \partial f(t,\theta)/\partial\theta$, considering both explicit and implicit dependencies between function $f(t,\theta)$ and parameter θ.

2.1 DDM for general response sensitivity calculation

The DDM differentiates analytically the space- and time- discretized equations of motion governing the dynamic systems with respect to the model or loading parameters. At each time or load step, the consistent FE response sensitivities using DDM are computed after convergence is reached and before the response state is committed. In the context of FE response analysis, after spatial discretization, the partial differential equation governing the motion of the structural and/or geotechnical system takes the form,

$$\boldsymbol{M}(\theta)\ddot{\boldsymbol{u}}(t,\theta) + \boldsymbol{C}(\theta)\dot{\boldsymbol{u}}(t,\theta) + \boldsymbol{R}\left(\boldsymbol{u}(t,\theta),\theta\right) = \boldsymbol{F}(t,\theta) \tag{2}$$

where $\boldsymbol{M}$ = the mass matrix, $\boldsymbol{C}$ = the damping matrix, $\boldsymbol{R}\left(\boldsymbol{u}(t,\theta),\theta\right)$ = the inelastic restoring force, $\boldsymbol{F}(t,\theta)$ = the dynamic load applied, $\boldsymbol{u}(t,\theta)$ = the nodal displacement vector, t = time and the superposed dot operator = differentiation with respect to time, and θ = the vector of model parameters for sensitivity analysis. The dynamic equation can be further discretized along time space using numerical integration method (e.g., Newmark – β method) widely used in structural dynamics (Chopra, 1995). A residual equation of motion in the discretized form need to be solved:

$$\begin{aligned}&\boldsymbol{\Psi}\left(\boldsymbol{u}_{n+1}(\theta,t)\right) = \tilde{\boldsymbol{F}}_{n+1}(\theta,t) - \\ &\left[1/\beta(\Delta t)^2\,\boldsymbol{M}(\theta)\boldsymbol{u}_{n+1}(\theta,t) + \alpha/\beta(\Delta t)\boldsymbol{C}(\theta)\boldsymbol{u}_{n+1}(\theta,t) + \boldsymbol{R}(\boldsymbol{u}_{n+1}(\theta,t),\theta)\right] = \boldsymbol{0}\end{aligned} \tag{3}$$

in which

$$\begin{aligned}&\tilde{\boldsymbol{F}}_{n+1}(\theta,t) = \boldsymbol{F}_{n+1}(\theta,t) + \boldsymbol{M}(\theta,t)\cdot \\ &\left[1/\beta(\Delta t)^2\,\boldsymbol{u}_n(\theta,t) + 1/\beta(\Delta t)\dot{\boldsymbol{u}}_n(\theta,t) - (1-1/2\beta)\ddot{\boldsymbol{u}}_n(\theta,t)\right] + \\ &\boldsymbol{C}(\theta,t)\left[\alpha/\beta(\Delta t)\boldsymbol{u}_n(\theta,t) - (1-\alpha/\beta)\dot{\boldsymbol{u}}_n(\theta,t) - (\Delta t)(1-\alpha/2\beta)\ddot{\boldsymbol{u}}_n(\theta,t)\right]\end{aligned} \tag{4}$$

The unknown nodal displacement vector at discrete time t = (n+1)Δt, $\boldsymbol{u}_{n+1}(\theta,t)$, where Δ$t$ denotes the constant integration time step, can be solved by driving the dynamic residual at discrete time t = (n+1)Δt to zero ($\boldsymbol{\Psi}\left(\boldsymbol{u}_{n+1}(\theta,t)\right) = \boldsymbol{0}$) using iterative methods, e.g., the incremental Newton-Raphson algorithm (Simo and Hughes, 1998).

In the following sections, the dependency of responses and parameters on time t and θ is dropped for convenience. After $\boldsymbol{\Psi}\left(\boldsymbol{u}_{n+1}\right)$ is driven to zero approximately such that the tolerance criteria is satisfied, Eq. (3) can be analytically differentiated with respect to θ, leading to the basic response sensitivity equation as (the unknown response sensitivity $\partial\boldsymbol{u}_{n+1}/\partial\theta$ is to be solved),

$$\begin{aligned}&\left[1/\beta(\Delta t)^2\cdot\boldsymbol{M} + \alpha/\beta(\Delta t)\cdot\boldsymbol{C} + \left(\boldsymbol{K}_T^{\text{stat}}\right)_{n+1}\right]\partial\boldsymbol{u}_{n+1}/\partial\theta = \\ &-\left(1/\beta(\Delta t)^2\,\partial\boldsymbol{M}/\partial\theta + \alpha/\beta(\Delta t)\cdot\partial\boldsymbol{C}/\partial\theta\right)\boldsymbol{u}_{n+1} - \\ &\partial\boldsymbol{R}\left(\boldsymbol{u}_{n+1}(\theta),\theta\right)/\partial\theta\,|_{\boldsymbol{u}_{n+1}} + \partial\tilde{\boldsymbol{F}}_{n+1}/\partial\theta\end{aligned} \tag{5}$$

In Eq. (5), the derivatives of most terms (e.g., $\partial \tilde{\boldsymbol{F}}_{n+1}/\partial\theta$) can be computed relatively straightforwardly, except for the internal force sensitivity $\partial \boldsymbol{R}\left(\boldsymbol{u}_{n+1}(\theta),\theta\right)/\partial\theta|_{\boldsymbol{u}_{n+1}}$. The notation $|_{\boldsymbol{u}_{n+1}}$ denotes the condition that the displacement vector $\boldsymbol{u}(t,\theta)$ is fixed. Since the internal forces $\boldsymbol{R}$ are assembled using element nodal forces, the calculation of $\partial \boldsymbol{R}\left(\boldsymbol{u}_{n+1}(\theta),\theta\right)/\partial\theta|_{\boldsymbol{u}_{n+1}}$ at the structural level depends on the element type (e.g., frame-type elements, the quad element for soil domain). The sensitivity of element nodal forces (at element level) needs to be calculated, which requires the sensitivities of section forces (at section level) and of stresses at each integration point (at material level). Therefore, each hierarchy in the nonlinear FE analysis framework needs to be differentiated with respect to θ, in order to form the $\partial \boldsymbol{R}\left(\boldsymbol{u}_{n+1}(\theta),\theta\right)/\partial\theta|_{\boldsymbol{u}_{n+1}}$ in Eq. (5). Taking advantage of the software architecture of *OpenSees*, the algorithms of DDM have been implemented by authors and coworkers at various hierarchies of the FE response calculations for the structural or geotechnical systems. The DDM is very accurate since it calculates an analytical solution for discretized equation of motion. The DDM is also highly efficient because the Eq. (5) can be solved with very limited computational cost, due to the fact that the dynamic consistent tangent stiffness matrix (on the left hand side of Eq. (5)) and its LU decomposition has already been obtained during the FE response analysis. A brief introduction is provided as follows, and readers can refer to the relative literatures for details (Zhang and Der Kiureghian, 1993; Kleiber *et al*., 1997; Conte *et al*., 2001, 2003; Gu and Conte, 2003, Li *et al*. 2017).

2.2 DDM for frame-type components in structural systems

In this section, the displacement-based beam-column element is used for the frame-type components, e.g., piles and piers in bridges, beams and columns in buildings. The derivative of the internal resisting force vector $\partial \boldsymbol{R}\left(\boldsymbol{u}_{n+1}(\theta),\theta\right)/\partial\theta|_{\boldsymbol{u}_{n+1}}$ in Eq. (5) can be directly assembled from the element resisting force derivatives,

$$\partial \boldsymbol{R}\left(\boldsymbol{u}_{n+1}(\theta),\theta\right)/\partial\theta\Big|_{\boldsymbol{u}_{n+1}} = \sum_{n=1}^{Nel}\left[\left(A_{\mathrm{b}}^{(\mathrm{e})}\right)^{\mathrm{T}} \Gamma_{\mathrm{REZ}}^{(\mathrm{e})\mathrm{T}}\ \Gamma_{\mathrm{ROT}}^{(\mathrm{e})\mathrm{T}}\ \Gamma_{\mathrm{RBM}}^{(\mathrm{e})\mathrm{T}} \cdot \int_{\Omega_{\mathrm{e}}} \boldsymbol{B}^{\mathrm{T}}(\boldsymbol{x})\cdot\partial\boldsymbol{\sigma}(\boldsymbol{x})/\partial\theta\big|_{\boldsymbol{\varepsilon}_{n+1}} \cdot \mathrm{d}\Omega_{\mathrm{e}}\right] \tag{6}$$

where, $A_{\mathrm{b}}^{(\mathrm{e})}$ is the Boolean localization matrix for element "e", $\Gamma_{\mathrm{REZ}}^{(\mathrm{e})\mathrm{T}}$, $\Gamma_{\mathrm{ROT}}^{(\mathrm{e})\mathrm{T}}$, $\Gamma_{\mathrm{RBM}}^{(\mathrm{e})\mathrm{T}}$ are the kinematic transformation matrices, where REZ accounts for the rigid end zone, ROT accounts for the rotation from global to local reference system, and RBM accounts for the rigid body modes (using the transformation from local to basic reference system), and $\boldsymbol{B}(\boldsymbol{x})$ is a transformation matrix between element displacement and strain. The response sensitivity calculation at the section and material level $\partial\boldsymbol{\sigma}(\boldsymbol{x})/\partial\theta$ depends on the type of sections or materials, therefore are not presented herein, but can be found in the literature (McKenna and Fenves, 2001; Barbato *et al*., 2010).

2.3 DDM for soil-foundation system

The DDM-based sensitivity algorithm has been extended to various 3D material models for soil-foundation systems in OpenSees, including the multi-yield surface J_2 plasticity clay soil model, the bounding surface sandy soil model, the truncated Drucker-Prager model, and the cap plasticity model. Readers of interest are referred to the literatures (Iwan, 1967; Mroz, 1967; Sandler *et al*., 1976; Prevost, 1977, 1978; Dafalias, 1986; Wang and Dafalias, 1990; Elgamal *et al*., 2003; Gu and Wang, 2013; Gu *et al*., 2009, 2010, 2015, 2016; Gao *et al*., 2015 ; Xie and Zhang, 2017)

3 Application examples

The SFSI during an earthquake process consists of the kinematic effects and the inertial effects. The input ground motion to the base of the structure will be different from rigid base excitation in terms of amplitude, frequency components, as well as the additional rotational component of the foundation. Including SFSI in the system response prediction and performance assessment is of significant importance, as explored in the literature (Goschy, 1978; Dutta and Roy, 2002; Liu, 2012). By accounting for the SFSI using continuum mechanics-based model of soil domain, the SFSI effects are addressed and its effects on the structural and geotechnical system responses can be studied. In this paper, instead of focusing on the response of SFSI systems subject to earthquakes, the response sensitivity to the SFSI model parameters is investigated. Two prototype SFSI systems are developed and analyzed in *OpenSees*, taking advantage of the fiber-based nonlinear beam-column elements for frames and the 3D constitutive models for the foundation and soil, as well as the associated DDM based FE response sensitivity analysis algorithms for SFSI systems.

3.1 A pile-supported bridge pier

In the context of bridge engineering, a pile-supported bridge pier column supported on a single pile embed in clay soil medium is studied, with the FE model shown in Fig.1(a). This SFSI system consists of the soil domain with dimensions 5.6 m × 2.0 m × 5.0 m, the reinforced-concrete (RC) pile with a circular cross section of a diameter 0.3 m, and the pier column with the same cross section as the pile (e.g., 1.0 m extension) and a lumped mass of 10.0 tons at the top. This pile-supported bridge pier column aims to represent the fundamental mode in the transverse direction of a bridge.

In the FE model of the SFSI system, the layered

soil medium is modeled using isoparametric four-node quadrilateral finite elements and a pressure-independent multi-yield surface J_2 plasticity constitutive model (Elgamal *et al*., 2003). The soil medium consists of five different soil layers and the variation of the soil properties is accounted through different material model parameters. The pile and the pier column are modeled using displacement-based Euler-Bernoulli beam-column elements with distributed plasticity (Fig. 1(b)). The cross sections are discretized into fibers with a specific nonlinear uniaxial material model assigned to each fiber. The uniaxial material models based on the Kent-Scott-Park model with zero tension stiffening (Scott *et al*. 1982), denoted as *concrete01* in OpenSees, with a compressive strength of 28.0 MPa and 34.0 MPa, are used for the unconfined concrete cover layer and the confined concrete core, respectively. The one-dimensional J_2 plasticity model *UniaxialJ2Plasticity*, with both kinematic and isotropic hardening (Barbato and Conte, 2006) and yield strength of 248.0 MPa, is used to model the reinforcing steel along longitudinal direction. Note that no sliding interface is modeled between the pile and soil here. However, quasi-rigid beam-column elements with exceedingly stiff properties (to represent the volume of the pile) are used to account for the geometric offset between the centroid of pile and the periphery of the pile, by connecting the periphery nodes of the quasi-rigid beam-column elements with the corresponding soil nodes at the periphery of the cross section of the pile (refer to C and E, D and F in Fig. 1a). Detailed material model parameters used in this SFSI system are shown in Table 1, and the response sensitivities to these parameters are investigated based on the DDM analysis of the FE model subject to an

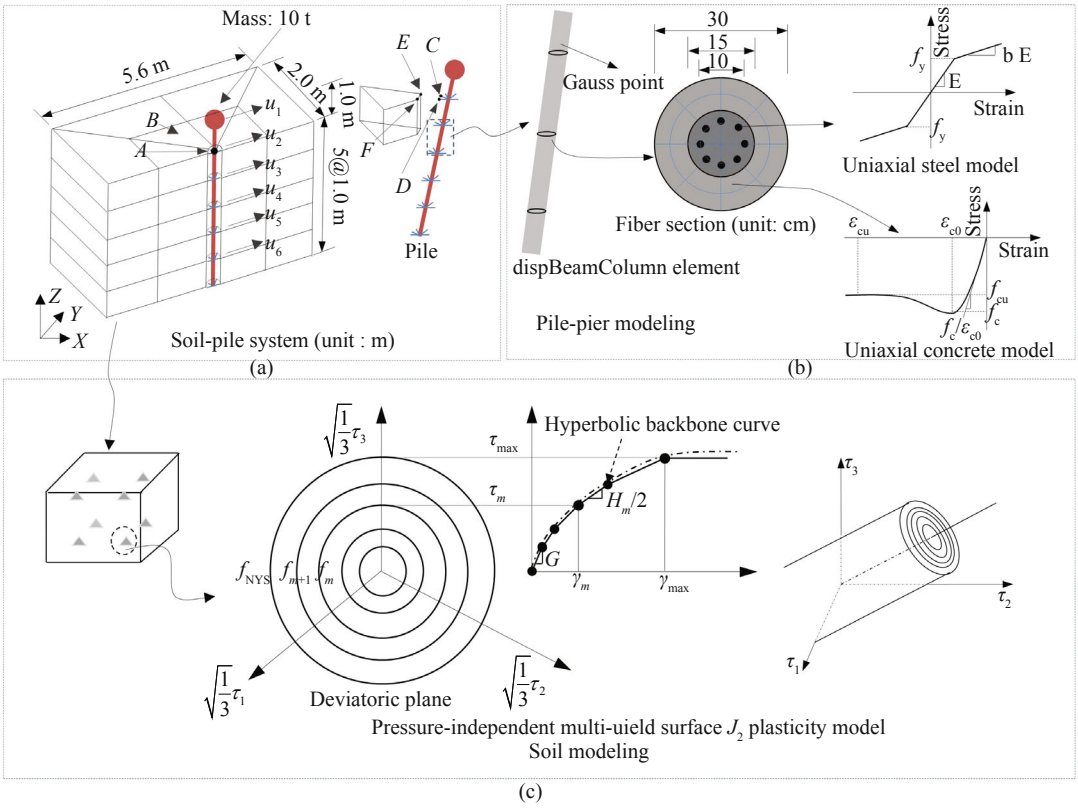

Fig. 1 FE modeling of the SFSI prototype for a pile-supported bridge pier: (a) isometric view, (b) pile-pier model using nonlinear fiber displacement beam-column element, (c) model of soil using brick element and multi-yield surface J_2 plasticity model

Table 1 Material model paramters used in the SFSI system prototype for a pile-supported bridge pier

Concrete			Reinforcing steel		Soil			
Para.	Core	Cover	Para.		Para.	G (kPa)	τ_{max} (kPa)	K (kPa)
f_c (kPa)	3.4×10^4	2.8×10^4	E (kPa)	2.10×10^8	#1: sand	5.445×10^4	33	1.6×10^5
f_{cu} (kPa)	2.4×10^4	0	f_y(kPa)	2.48×10^5	#2: sand	3.38×10^4	26	1.0×10^5
ε_{c0}	0.005	0.002	b	0.02	#3: sand	6.125×10^4	35	1.8×10^5
ε_{cu}	0.02	0.006	-	-	#4: sand	9.68×10^4	44	2.9×10^5
-	-	-	-	-	#5: pebble	1.8×10^5	60	5.4×10^5

earthquake ground excitation.

A simple shear condition for the soil domain is imposed by enforcing the same displacement response for the corresponding degree-of-freedom, in both the *x*- or *y*-directions, of the boundary nodes at the same depth. The seismic loading is applied to the SFSI system along the *x* axis in terms of uniform base excitation. For the purpose of illustration and validation, the north-south component of the 1940 Mw 6.9 Imperial Valley earthquake (denoted as the El Centro 1940) is used as the seismic input motion at the base of the SFSI system with a scale factor of 2.0, see Fig. 2, in order to develop significant nonlinearity in the model during the seismic excitation. The nominal dynamic integration time step is 0.01 seconds and adaptive time steps between 0.001 and 0.01 seconds are used to improve the convergence performance whenever necessary during the process of time history analysis in *OpenSees*.

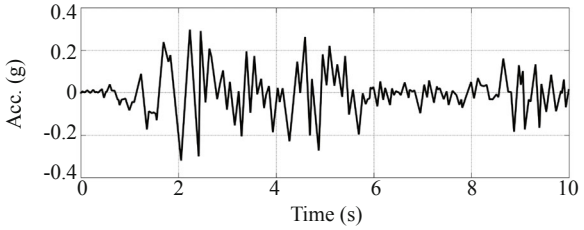

Fig. 2 Earthquake ground motion acceleration history (El Centro 1940, PGA = 0.326 g)

Under the imposed earthquake ground motion, the seismic response of the SFSI system is investigated in Figs. 3 and 4. Figure 3 shows the relative displacement of the SFSI system at various heights, including the displacements for the pier top u_1 and different soil layers with respect to the base (u_2, u_3, u_4, u_5, u_6, see Fig. 1(a)) . Large displacement of the pier top is due to the flexure deformation of the pier column, as well as the translational and rotational displacements at the column base (see Fig. 4(a)). Due to SFSI effects, the additional rotational component at the bottom of the pier at ground surface also contributes to the displacement at the pier top. Figure 4(b) shows the displacement envelope in the SFSI system. Under such a strong excitation, significant nonlinear behavior is observed through the moment-curvature response at the bottom section of the pier column (point *A* in Fig. 1(a)), as shown in Fig. 4(c). The soil layers experienced different levels of deformation, and significant nonlinearity can also be observed through the shear stress-strain responses for a representative point in the soil (point *B* in Fig. 1(a)), as shown in Fig. 4(d).

During the time history analysis of the SFSI system, the response sensitivities of pier top displacement with respect to model parameters are computed based on DDM sensitivity analysis. The parameters include those in reinforcing steel, cover concrete, core concrete,

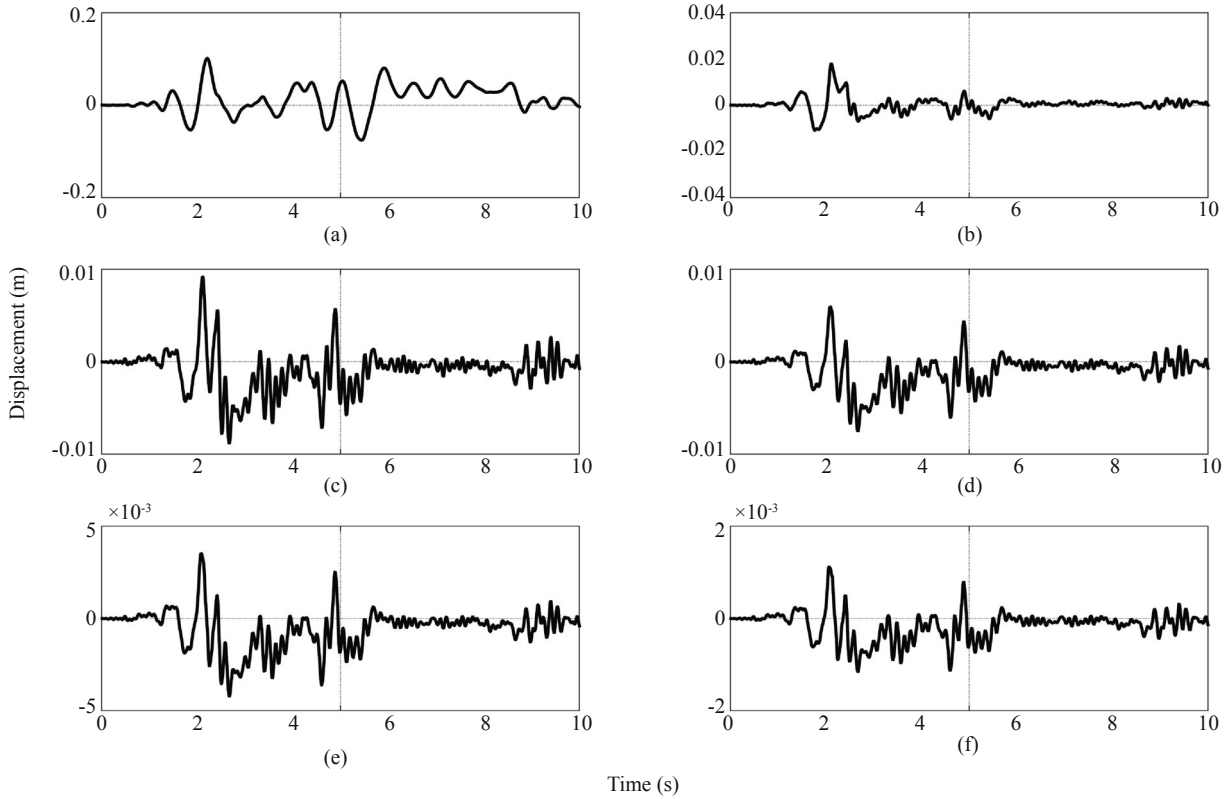

Fig. 3 Relative displacement responses of the SFSI system prototype for the pile-supported bridge pier subject to 1940 El Centro Earthquake (scaled by 2.0) for: (a) the pier top (u_1), (b) the top of soil layer #1(u_2), (c) the soil layer #2(u_3), (d) the soil layer #3(u_4), (e) the soil layer #4(u_5), (f) the soil layer #5(u_6)

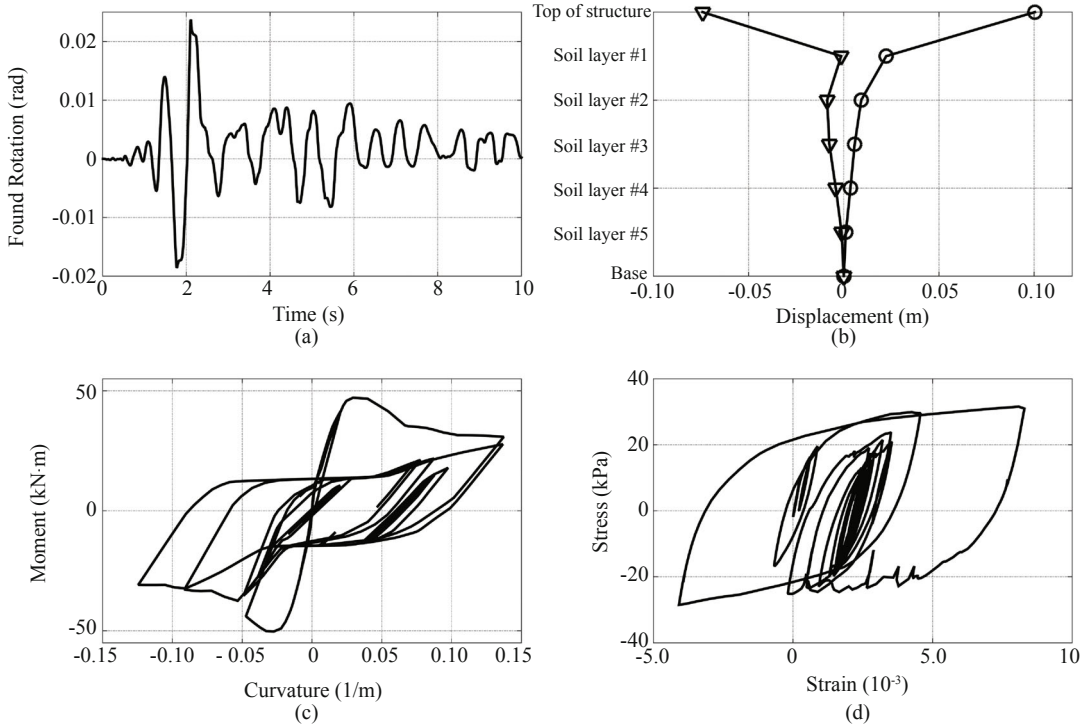

Fig. 4 (a) Rotation of the pile top at the base of the pier column, (b) displacement envelope along depth, (c) the moment-curvature response at the bottom section of the pier column (Point *A* in Fig. (1a)), (d) the shear stress-strain relationship for a representative point in the soil (Point *B* in Fig. (1a))

and soil. To verify the DDM results, the normalized sensitivity of the relative displacement at the pier top with respect to the strain at peak strength of core concrete, $(\partial u_1/\partial \varepsilon_{c0})\varepsilon_{c0}$, are studied in detail. The response sensitivity calculated by FFD with decreasingly small perturbations ($\Delta\theta/\theta$ from 10%, 1%, 0.1%, to 0.01%) are compared with the DDM results, as shown in Fig. 5. It shows that the response sensitivity obtained through FFD (with 10%, 1% and 0.1% perturbation) converges to the sensitivity analysis result obtained through DDM due to the reducing truncation error in FFD. However, further decreasing the perturbation of the sensitivity parameter to 0.01% leads to the 'divergence' of FFD sensitivity from DDM result, due to the round-off error in FFD. In some special cases, there will never be a suitable perturbation size, using which the FFD provides acceptable sensitivity approximation, and this is called the 'perturbation size dilemma'. The verification example using FFD shows an important advantage of DDM over FFD, that is, the DDM is insensitive to numerical noise. Through analysis not shown herein (Gu *et al*., 2013), the normalized sensitivity $(\partial r/\partial\theta)\theta$ by DDM has the same precision with the response r, while the accuracy of $(\Delta r/\Delta\theta)\theta$ by FFD is significantly worse than that of response r. The DDM is not only very accurate, but also highly efficient, able to save up to 40% CPU time over FFD for small scale problems. This advantage significantly increases with the scale of problems. Therefore the DDM is particularly suitable for large scale SFSI problems.

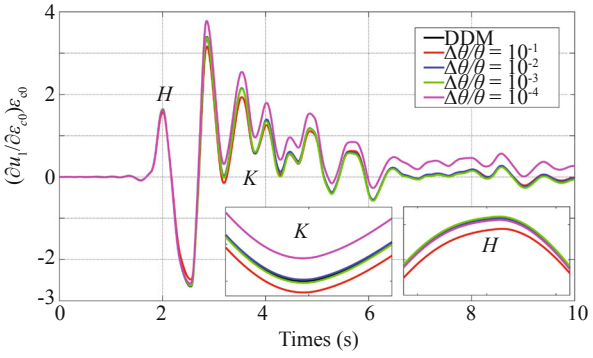

Fig. 5 Verification of the DDM-based response sensitivity using FFD in terms of $(\partial u_1/\partial \varepsilon_{c0})\varepsilon_{c0}$

The time histories of the normalized response sensitivity with respect to the five most sensitive parameters are presented in Fig. 6. These parameters are $f_{c,cover}$, $\varepsilon_{cu,cover}$, $\sigma_{y,steel}$, E_{steel}, $\varepsilon_{c0,cover}$. The cover concrete will be damaged and therefore is very sensitive on affecting the system responses. The steel properties are also relatively sensitive. The tornado plots for the sensitivity at the occurrence of the peak response sensitivities are presented in Fig. 7 for parameters in cover concrete, core concrete, steel and soil materials, respectively. It shows that different material parameters play significantly different roles in affecting the response quantities of interest (e.g., the pier top displacement). This standalone sensitivity analysis provides insightful guidance for the FE model updating or calibration, in sense of

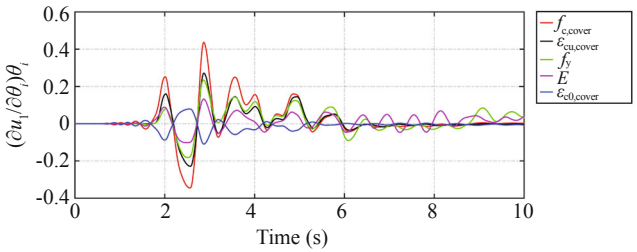

Fig. 6 The normalized response sensitivity with respect to the five most sensitive parameters

determining which parameters should be updated or calibrated. For this specific example, the most sensitive parameters in concrete cover, concrete core, steel and soil are almost the strength related parameters: $f_{c,cover}$, $f_{c,core}$, $\sigma_{y,steel}$, and G_1. Based on the studies not shown herein, the stiffness related parameters are more important for weak earthquake input, while the strength related parameters are dominant for strong earthquake input (Gu *et al*., 2013). Comparing the four groups of parameters in Fig. 7, it is observed that the parameters of cover concrete is the most sensitive and those of core concrete are least sensitive among all material parameters. A complete comparison of the normalized sensitivity of the top displacement with respect to all the sensitivity parameters is studied and the relative importance RI of parameters with decreasing importance is: (1) $f_{c,cover}$, (2) $\varepsilon_{cu,cover}$, (3) $\sigma_{y,steel}$, (4) E_{steel}, (5) $\varepsilon_{c0,cover}$, (6) G_1, (7) $\tau_{max,1}$, (8) G_2, (9) $\tau_{max,2}$, (10) G_3, (11) G_4, (12) $f_{c,core}$, (13) G_5, (14) $\varepsilon_{c0,core}$, (15) $\tau_{max,4}$, (16) $\tau_{max,3}$, (17) b, (18) $\tau_{max,5}$, (19) $f_{cu,core}$, (20) $\varepsilon_{cu,core}$.

3.2 A pile-supported RC frame building

The second application example used in this paper is a SFSI system prototype for a pile-supported 3D RC frame building structure, with each of the four frame columns at the ground surface supported on a single-pile foundation. This building is a 3-story 1-by-1-bay RC frame with concrete slabs at each floor as shown in Fig. 8(a), subject to the earthquake ground motion input in both x-direction and y-direction, shown in Fig. 8(b) and (c) respectively. The dimensions of the building frame are also shown in Fig. 8(a), with the same story height h = 3.66 m and floor dimension of 6.10 m × 6.10 m. The piles embedded in soil are 4.0 m deep below the ground surface and assumed to have the dimension and material properties as the frame columns.

Nonlinear seismic response of the SFSI system is simulated using a nonlinear FE model with the frame modeled using displacement-based Euler-Bernoulli beam-column elements with distributed plasticity developed in *OpenSees* (Mazzoni *et al*., 2006). These elements with fiber-discretized cross sections (represented by integration points) are used to characterize the spread of plastic regions along the element length. More details about distributed-plasticity FE models using displacement-based beam-column elements can be found in Taucer *et al*. (1991). The nonlinear material behavior of each fiber of the discretized RC section is defined by uniaxial material constitutive laws for the concrete and the bilinear hysteretic model for the reinforcing steel. The concrete slabs are modeled through a rigid diaphragm constraint at each floor to impose rigid in-plane behavior.

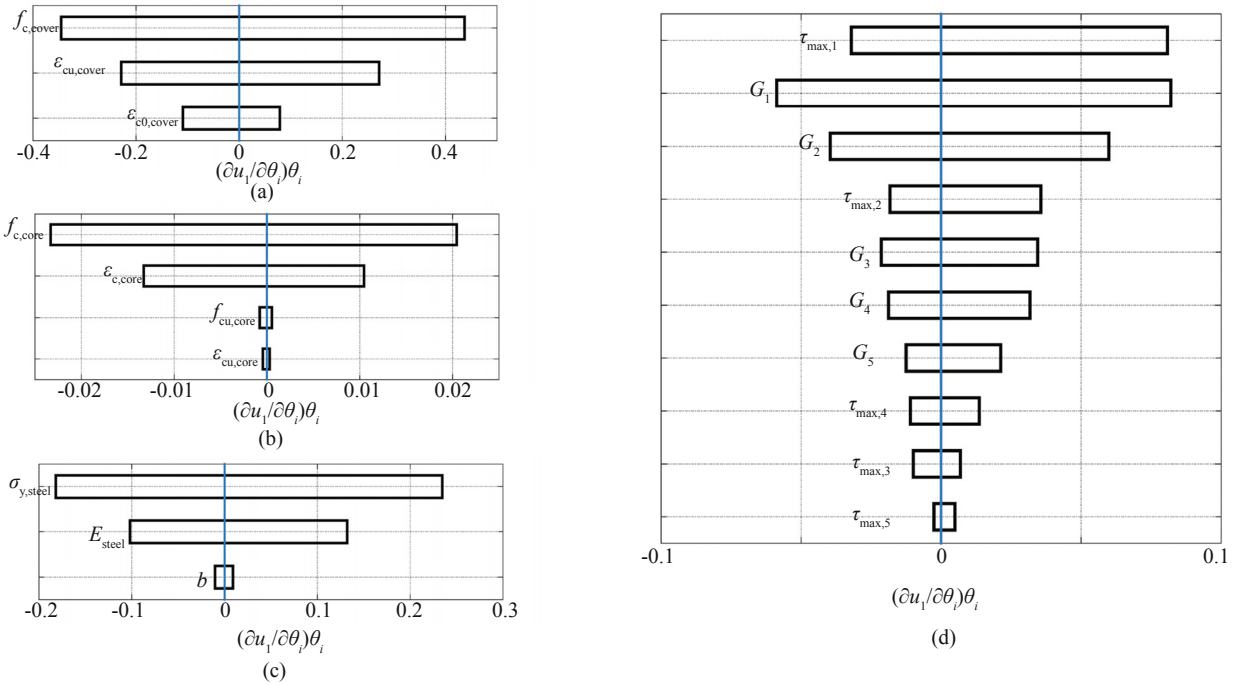

Fig. 7 Tornado plots for the normalized sensitivity at the occurrence of the peak response sensitivity: (a) concrete cover material parameters, (b) core concrete material parameters, (c) steel model parameters, (d) soil layer parameters

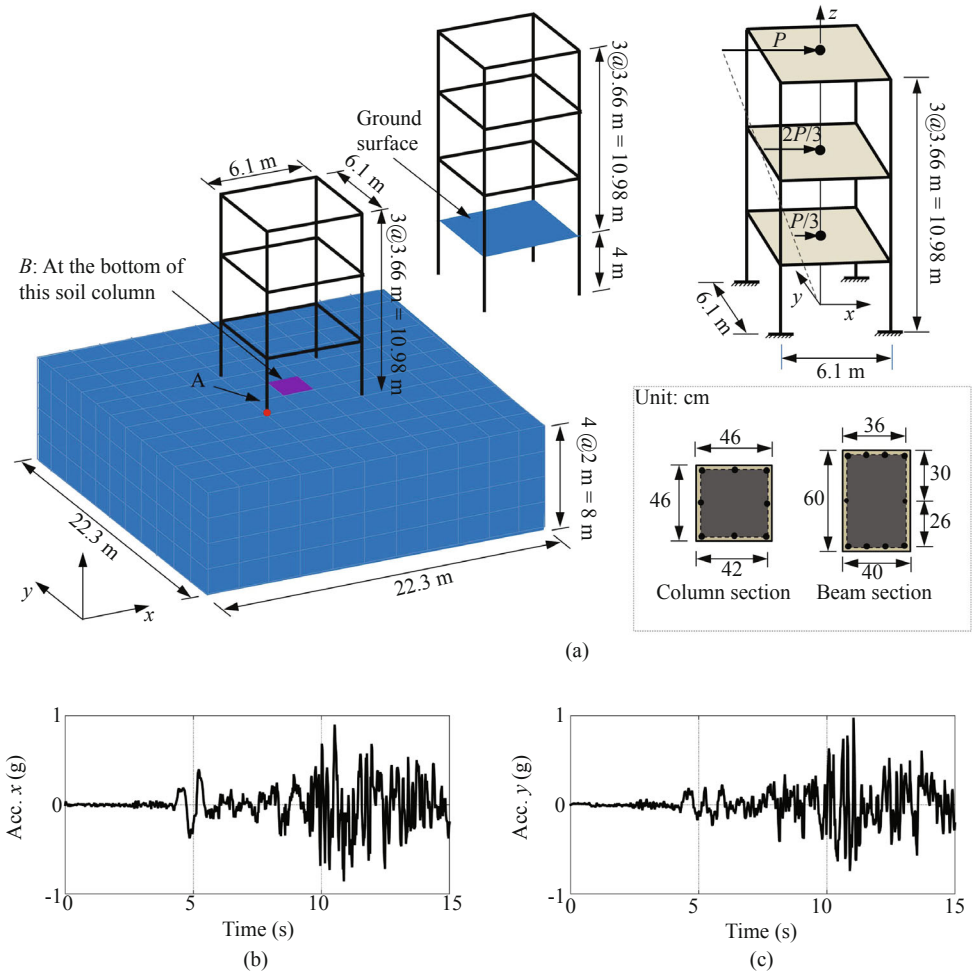

Fig. 8 The FE model of the SFSI prototype for a RC frame building: (a) the modeling details, (b) the earthquake ground motion input in *x*-direction, (c) the earthquake ground motion input in *y*-direction

In the SFSI system, the soil domain of dimension 22.3 m × 22.3 m × 8 m is accounted and modeled using a pressure-independent multi-yield surface J_2 plasticity constitutive model (Elgamal *et al*., 2003). The embedded pile is represented in the same manner as described in the previous example. The same simple shear condition for the soil domain as in example 1 is used by enforcing the same response for corresponding degree-of-freedom, in both the *x*- or *y*-directions, of all the boundary nodes with the same depth. In this application, bidirectional horizontal earthquake excitations (the 1978 Tabas Earthquake) are applied, with the fault-normal component imposed in the *x*-direction and fault-parallel component imposed in the *y*-direction. The peak ground acceleration (PGA) for both components are scaled up close to 1.0 g to excite the SFSI system and make it significantly yield.

Figure 9 shows the global and the local responses of the SFSI system considered here. Figure 9(a) shows the envelop of the relative displacements (with respect to the bottom of soil) of the soil layers and frame structure in both the *x*-direction and *y*-direction. The soil in the *y*-direction deformed more than the *x*-direction, while the structure deformed more in the *x*-direction, and this is mainly due to the dynamic properties in the soil and structure as well as the frequency and amplitude properties in the seismic input. Figure 9(b) shows the moment curvature behavior of the bottom section of a corner column (point *A* in Fig. 8(a)). The column experienced significant nonlinearity in both directions. Similarly, the nonlinearity in the soil domain can be observed in Fig. 9(c), which shows the shear stress – strain behavior during the earthquake excitation for the soil located at the point *B* (see Fig. 8(a)). Under this earthquake ground motion excitation, the SFSI system has yielded in both the structure and the soil.

Further verification of DDM is performed using FFD based on this SFSI system, shown in Fig. 10. The difficulty of choosing the appropriate perturbation of parameters in FFD tends to be problematic, because of the dilemma of the perturbation size. The perturbation cannot be too large or too small because of the truncation error and round-off error, which is particularly true for large complicated nonlinear SFSI systems.

Figure 11 shows the time histories of the normalized response sensitivity with respect to the four most sensitive parameters for the SFSI system: $\tau_{\max,4}$, E_{col}, $\tau_{\max,3}$, $f_{\text{y,steel}}$.

Figure 12 summaries the normalized response sensitivity at the occurrence of the peak response

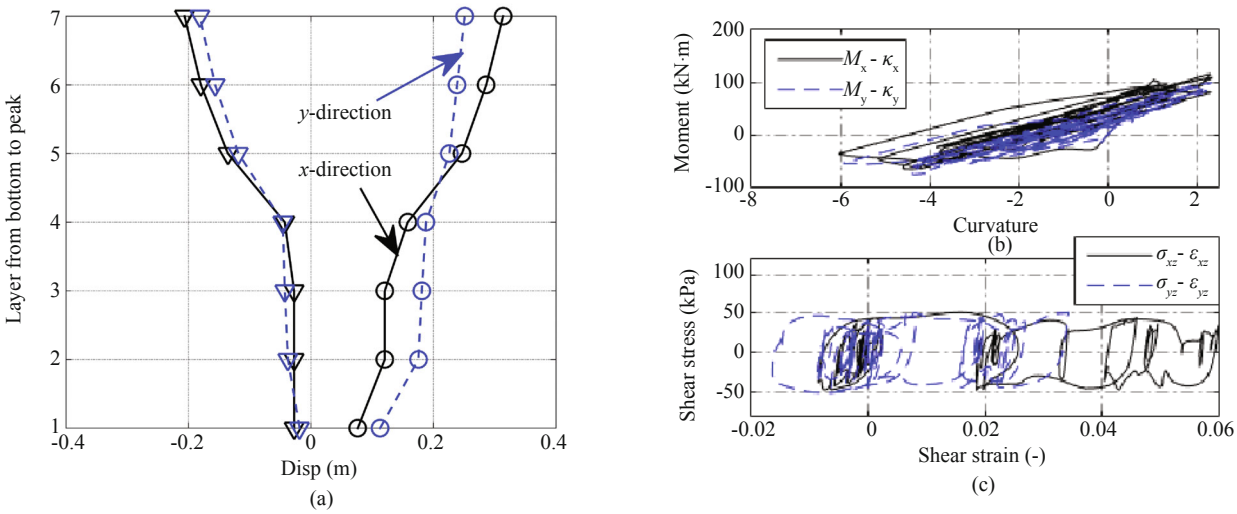

Fig. 9 (a) Displacement envelope of the SFSI system prototype for the pile-supported building frame subject to the 1978 Tabas Earthquake, (b) the moment-curvature response at the bottom section (located at point *A* in Fig. 8(a)) of the pier column, (c) the shear stress-strain relationship for a representative (located at point *B* in Fig. 8(a)) in the soil

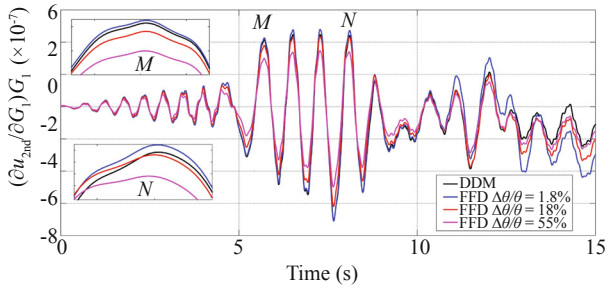

Fig. 10 Verification of the DDM-based response sensitivity using FFD in terms of the normalized sensitivity of the second floor displacement with respect to G_1

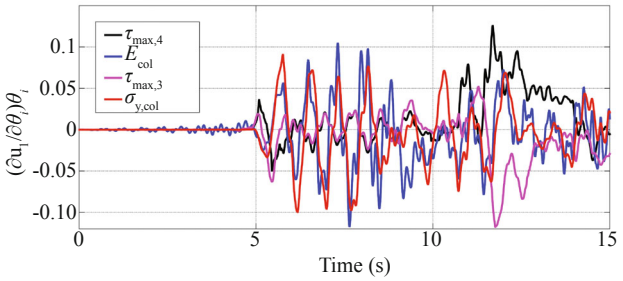

Fig. 11 The normalized response sensitivity with respect to the four most sensitive parameters for the SFSI system prototype of pile-supported building frame

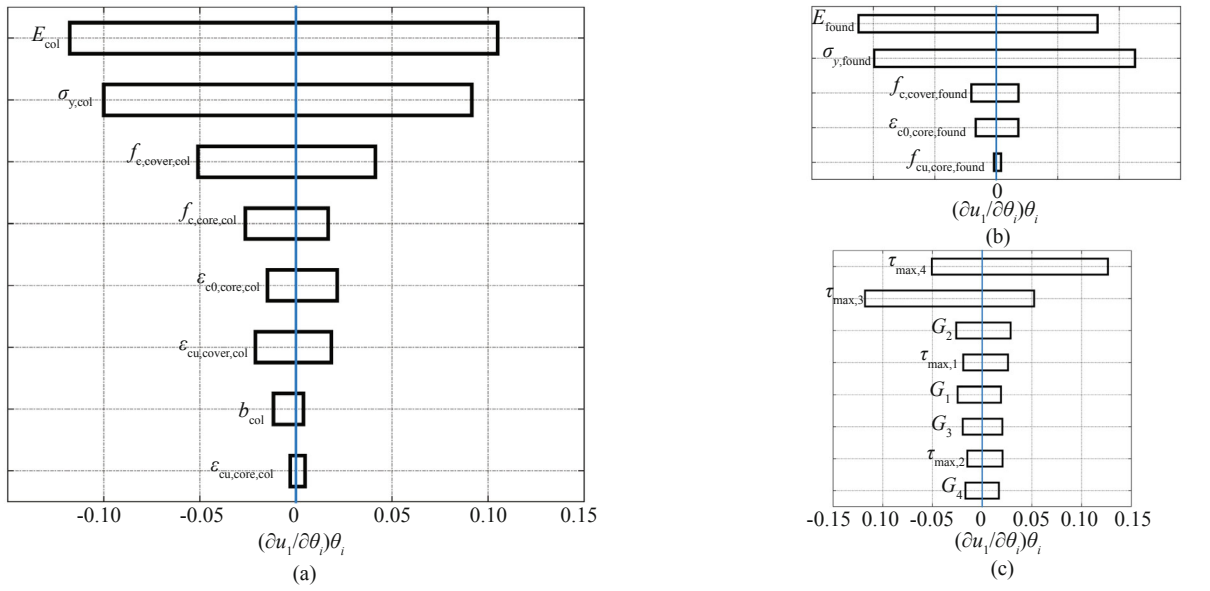

Fig. 12 The tornado plot of normalized response sensitivity at the occurrence of the peak response sensitivity: (a) building frame parameters, (b) the foundation parameters, (c) soil parameters

sensitivity with respect to the building frame parameters, the foundation parameters, and the soil parameters, respectively. It is clear that the three parameters, $\tau_{max,4}$, $E_{foundation,steel}$, and $\tau_{max,4}$ are most sensitive parameters of the structure, foundation and soil, respectively, while the parameters in foundation is much less sensitive than those in structure or soil.

Comparing the normalized sensitivity of the top displacement in both *x*- and *y*-directions with respect to all the sensitivity parameters considered here, the relative importance RI of these 23 material parameters on the top displacement in the *x*-direction with decreasing importance is: (1) $\tau_{max,4}$, (2) E_{steel}, (3) $\tau_{max,3}$, (4) $\sigma_{y,steel}$, (5) $f_{c,cover}$, (6) $f_{c,core}$, (7) G_2, (8) $\tau_{max,1}$, (9) G_1, (10) $E_{foundation,steel}$, (11) $\sigma_{y,foundation,steel}$, (12) $\varepsilon_{c0,core}$, (13) $\varepsilon_{c0,cover}$, (14) G_3, (15) $\tau_{max,2}$, (16) G_4, (17) $\varepsilon_{cu,cover}$, (18) b_{steel}, (19) $f_{cu,core,foundation}$, (20) $\varepsilon_{c0,core,foundation}$, (21) $b_{foundation,steel}$, (22) $f_{cu,core}$, (23) $\varepsilon_{cu,core}$. The RI of these 23 material parameters on the top displacement in the *y*-direction with decreasing importance is: (1) $\sigma_{y,steel}$, (2) $\tau_{max,4}$, (3) E_{steel}, (4) $\tau_{max,3}$, (5) $f_{c,core}$, (6) $f_{c,cover}$, (7) $\tau_{max,1}$, (8) $\sigma_{y,foundation,steel}$, (9) G_2, (10) $\tau_{max,2}$, (11) G_3, (12) $E_{foundation,steel}$, (13) G_4, (14) $\varepsilon_{cu,cover}$, (15) $\varepsilon_{c0,core}$, (16) G_1, (17) $\varepsilon_{c0,cover}$, (18) b_{steel}, (19) $f_{c,core,foundation}$, (20) $\varepsilon_{c0,core,foundation}$, (21) $b_{foundation,steel}$, (22) $f_{cu,core}$, (23) $\varepsilon_{cu,core}$. The stand-alone sensitivity analysis for such SFSI systems provided invaluable information of gradient information of the system response, which can be used for further FE model updating studies for SFSI systems.

4 Conclusions

With the emerging need of computing efficient and accurate response sensitivities, the direct differential method (DDM) has been developed for both structural and geotechnical systems. This paper presented the fundamental theory of DDM, the advantages of DDM in the sense of accuracy and efficiency over other gradient computation methods, the extension of DDM to various constraints, elements, sections and materials, and their applications to sensitivity analysis of complicated three-dimensional soil-foundation-structure interaction (SFSI). Two prototype systems (one for a pile-supported bridge pier column, and the other for a pile-supported RC building frame) are used to investigate the response sensitivity with respect to various parameters in the structure, foundation and soil materials. The forward finite difference (FFD) method is used to validate DDM through the asymptotically convergence of FFD-based sensitivity with increasingly small perturbations, and the selection of perturbation size is discussed based on error analysis for FFD. The comparison between DDM and FFD demonstrates the advantages of DDM (e.g., accurate, efficient, insensitivity to numerical noise). Furthermore, the relative importance and effects of the model parameters of structure, foundation and soil materials on the responses of SFSI systems are investigated by taking advantage of the sensitivity analysis results. The extension of DDM to SFSI systems will boost the other hotspot research topics based on FE analysis and gradient-based algorithms, e.g. FE model updating and nonlinear system identification of complicated SFSI systems.

Acknowledgement

The authors acknowledge the financial supports from the National Key Research and Development Program of China with Grant No. 2016YFC0701106. The corresponding author acknowledges the support provided by the Natural Sciences and Engineering Research Council of Canada via Discovery Grant (NSERC RGPIN-2017-05556 Li).

References

Barbato M and Conte JP (2005), "Finite Element Response Sensitivity Analysis: a Comparison Between Force-Based and Displacement-Based Frame Element Models," *Computer Methods in Applied Mechanics and Engineering*, **194**(12): 1479–1512.

Barbato M and Conte JP (2006), "Finite Element Structural Response Sensitivity and Reliability Analyses Using Smooth Versus Non-Smooth Material Constitutive Models" *International J. of Reliability and Safety*, **1**(1-2): 3–39.

Barbato M, Gu Q, and Conte JP (2010), "Probabilistic Pushover Analysis of Structural and Soil-Structure Systems," *Journal of Structural Engineering*, **136**(11): 1330–1341.

Ciampoli M and Pinto PE (1995), "Effects of Soil-Structure Interaction on Inelastic Seismic Response of Bridge Piers," *J. of Structural Engineering*, **121**(5): 806–814.

Conte JP, Barbato M and Spacone E (2004), "Finite Element Response Sensitivity Analysis Using Force-Based Frame Models," *International Journal for Numerical Methods in Engineering*, **59**(13): 1781–1820.

Conte JP, Vijalapura PK and Meghella M (2003), "Consistent Finite-Element Response Sensitivity Analysis," *J. of Engineering Mechanics*, *ASCE*, **129**(12): 1380–1393.

Conte JP (2001), "Finite Element Response Sensitivity Analysis in Earthquake Engineering," *Earthquake Engineering Frontiers in the New Millennium*, Spencer & Hu, Swets & Zeitlinger, 395–401.

Chopra AK, (1995), "*Dynamics of Structures*," New Jersey: Prentice Hall, 1995.

Dafalias YF(1986), "Bounding Surface Plasticity. I: Mathematical Foundation and Hypoplasticity," *J. of Engineering Mechanics*, *ASCE*, **112**(9): 966–987.

Ditlevsen O, and Madsen HO (1996), *Structural Reliability Methods*, Wiley, New York.

Doebling SW, Farrar CR, Prime MB, *et al*. (1996), "Damage Identification and Health Monitoring of Structural and Mechanical Systems from Changes in Their Vibration Characteristics: A Literature Review," *Los Alamos National Lab.*, NM (United States).

Dolšek M and Fajfar P (2007), "Simplified Probabilistic Seismic Performance Assessment of Plan-Asymmetric Buildings," *Earthquake Engineering & Structural Dynamics*, **36**(13): 2021–2041.

Dutta SC and Roy R (2002), "A Critical Review on Idealization and Modeling for Interaction among Soil–Foundation–Structure System," *Computers & Structures*, **80**(20): 1579–1594.

Elgamal A, Yang Z, Parra E, *et al*.,(2003), "Modeling of Cyclic Mobility in Saturated Cohesionless Soils," *International Journal of Plasticity*, **19**(6): 883–905.

Gao Y, Gu Q and Qiu ZJ (2015), "Sensitivity Analysis for Seismic Responses of Coupled Dam-Reservoir-Foundation Systems, under Review," *Journal of Engineering Mechanics, ASCE*. (Submitted)

Goschy B (1978), "Soil-Foundation-Structure-Interaction," *J. of the Structural Division*, **104**(5): 749–761.

Gu Q (2008), "Finite Element Response Sensitivity and Reliability Analysis of Soil-foundation-structure-Interaction (SFSI) Systems," *PhD Dissertation,* University of California San Diego, 2008.

Gu Q and Conte JP (2003), "Convergence Studies in Non-linear Finite Element Response Sensitivity Analysis," *Proceedings of ICASP9*, Berkeley, USA.

Gu Q, Conte JP, Yang Z and Elgamal A(2011), "Consistent Tangent Operator For a Multiyield-surface J2 Plasticity model," *Computational Mechanics*, *ASCE* **48**(1): 97–120.

Gu Q, Barbato M, Conte JP, *et al*. (2011), "OpenSees-SNOPT Framework for Finite-Element-Based Optimization of Structural and Geotechnical Systems" *J. of Structural Engineering*, **138**(6): 822–834.

Gu Q, Barbato M and Conte JP (2009), "Handling of Constraints in Finite-element Response Sensitivity Analysis," *J. of Engineering Mechanics*, **135**(12): 1427–1438.

Gu Q and Wang G (2013), "Direct Differentiation Method for Response Sensitivity Analysis of a Bounding Surface Plasticity Soil Model," *Soil Dynamics and Earthquake Engineering*, **49**: 135–145.

Gu Q, Vijalapura P and Qiu ZJ (2015), "Consistent Finite Element Response Sensitivity Analysis: Application to a Multi-Surface Cap Plasticity Model" *to be Submitted to Comupter Methods in Applied Mechanics and Engineering*.

Haber R and Unbehauen H (1990), "Structure Identification of Nonlinear Dynamic Systems—a Survey on Input/ Output Approaches,"*Automatica*, **26**(4): 651–677.

Iwan WD (1967), "On a Class of Models for the Yielding Behavior of Continuous and Composite Systems," *J. of Applied Mechanics*, **34**(3): 612–617.

Jae-Kwang Yang, Long-Yang Li and Sung-Soo Park (2017), "Sensitivity Analysis for Axis Rotation Diagrid Structural Systems According to Brace Angle Changes" *Earthquake Engineering and Engineering Vibration*, **16**(4): 783–791.

Kala, Zdeněk, and J Valeš (2017), "Global Sensitivity Analysis of Lateral-Torsional Buckling Resistance Based on Finite Element Simulations," *Engineering Structures*, **134**(1): 37–47.

Karoumi R (1999), "Some Modeling Aspects in the Nonlinear Finite Element Analysis of Cable Supported Bridges," *Computers & Structures*, **71**(4): 397–412.

Kleiber M, Antunez H, Hien TD, *et al*. (1997), *Parameter Sensitivity in Nonlinear Mechanics: Theory and Finite Element Computations*, Wiley, New York.

Kleiber M and Hien TD (1992), "The Stochastic Finite Element Method," *Basic Perturbation Technique and Computer Implementation*, Wiley, New York.

Kunnath SK, Larson L and Miranda E (2006), "Modeling Considerations in Probabilistic Performance-Based Seismic Evaluation: Case Study of the I-880 Viaduct," *Earthquake engineering & structural dynamics*, **35**(1): 57–75.

Liu H (2012), "Soil-Structure Interaction and Failure of Cast-Iron Subway Tunnels Subjected to Medium Internal Blast Loading," *J. of Performance of Constructed Facilities*, **26**(5): 691–701.

Zoutat M, Elachachi SM, Mekki M and Hamane M (2016), "Global Sensitivity Analysis of Soil Structure Interaction System Using N2-SSI Method," *European Journal of Environmental and Civil Engineering*, **22**(2): 192–211.

Mazzoni S, McKenna F, Scott MH *et al*. (2006), "OpenSees Command Language Manual," *Pacific Earthquake Engineering Research (PEER) Center*.

Mazzoni S, McKenna F, Scott MH, *et al*. (2004), *OpenSees Users Manual*, University of California, Berkeley , PEER.

McKenna F and Fenves GL (2001), *The OpenSees Command Language Manual*, University of California, Berkeley (*opensees.ce.berkeley.edu*).

Mroz Z (1967), "On the Description of Anisotropic Workhardening," *J. of the Mechanics and Physics of Solids*, **15**(3): 163–175.

Nelles O (2001), "Nonlinear System Identification: from Classical Approaches to Neural Networks and Fuzzy Models," *Springer Science & Business Media*.

Perić D, Owen DRJ and Honnor ME (1992), "A Model for Finite Strain Elasto-Plasticity Based on Logarithmic Strains: Computational Issues," *Computer Methods in Applied Mechanics and Engineering*, **94**(1): 35–61.

Prevost JH (1977), "Mathematical Modeling of

Monotonic and Cyclic Undrained Clay Behaviour," *International J. for Numerical and Analytical Methods in Geomechanics*, **1**(2): 195–216.

Prevost JH (1978), "Plasticity Theory for Soil Stress-Strain Behavior," *Journal of the Engineering Mechanics Division*, *ASCE*, **104**(EM5): 1177–1194.

Randal Fielder, Arturo Montoya, Harry Millwater and Patrick Golden (2017), "Residual Stress Sensitivity Analysis Using a Complex Variable Finite Element Method," *International Journal of Mechanical Sciences*, **133**(1): 112–120.

Sandler IS, Baladi GY and DiMaggio FL (1976), "Generalized Cap Model for Geological Materials," *J. of the Geotechnical Engineering Division*, **102**(7): 683–699.

Scott BD, Park R and Priestley MJN (1982), "Stress–Strain Behavior of Concrete Confined by Overlapping Hoops at Low and High Strain Rates," *ACI Journal*, **79**(1): 13–27.

Singhal A and Kiremidjian AS (1996), "Method for Probabilistic Evaluation of Seismic Structural Damage," *J. of Structural Engineering*, **122**(12): 1459–1467.

Simo JC and Hughes TJR (1998), *Computational Plasticity*. Springer, New York.

Taucer FF, Spacone E and Filippou FC (1991), "A Fiber Beam-Column Element for Seismic Response Analysis of Reinforced Concrete Structures," *Report 91/17*, *EERC,* Earthquake Engineering Research Center (EERC), University of California, Berkeley.

Ueno K and Liu YK (1987), "A Three-Dimensional Nonlinear Finite Element Model of Lumbar Intervertebral Joint in Torsion," *J.of Biomechanical Engineering*, **109**(3): 200–209.

Wang ZL and Dafalias YF (1990), "Bounding Surface Hypoplasticity Model for Sand," *J. of Engineering Mechanics*, *ASCE*, **116**(5): 983–1002.

Xie Zhinan and Zhang Xubin (2017), "Analysis of High-Frequency Local Coupling Instability Induced by Multi-Transmitting Formula – P-SV Wave Simulation in a 2D Waveguide," *Earthquake Engineering and Engineering Vibration*, **16**(1): 1–10.

Yao JT (1972), "Concept of Structural control," *J. of the Structural Division*, **98**(7): 1567–1574.

Zhang Y and Der Kiureghian A (1993), "Dynamic Response Sensitivity of Inelastic Structures," *Computer Methods in Applied Mechanics and Engineering*, **108**(1): 23–36.

Zona A, Barbato M and Conte JP (2005), "Finite Element Response Sensitivity Analysis of Steel-Concrete Composite Beams with Deformable Shear Connection," *J. of Engineering Mechanics*, *ASCE*, in press.

Zou Y, Tong L and Steven GP (2000), "Vibration-Based Model-Dependent Damage (Delamination) Identification and Health Monitoring for Composite Structures - a Review," *J. of Sound and Vibration*, **230**(2): 357–378.